




Laser induced modification of nickel surface for non-enzymatic glucose detection

A.S. Kondrateva ¹ ✉, D.A. Strekalovskaya ², B.V. Babuyk², A. Kuznetsov¹,
L.A. Filatov², P.G. Gabdullin ²

¹ St. Petersburg Academic University of the Russian Academy of Sciences, St. Petersburg, Russia

² Peter the Great St. Petersburg Polytechnic University, St. Petersburg, Russia

✉ freyanasty@ya.ru

Abstract. This article proposes for consideration the experimental results of applying the method of laser surface modification for the manufacture of a highly sensitive enzyme-free sensitive layer of the working electrode of a glucose sensor using nickel oxide as an example. This technology can be integrated into the lab-on-a-chip concept. Using cyclic voltammetry, the sensitivity of the proposed system to the addition of microdoses of glucose to the solution for unmodified and laser-modified nickel surfaces was studied. The formed structure of metal oxide sensors was studied for the determination of D-(+)-glucose in the range of analyte concentrations up to 1.5 μM . In addition, the sensitive layers made using the proposed technology showed durability and reproducibility of properties. This allows us to conclude that the demonstrated method of laser-induced metal surface modification is suitable for the production of a wide range of enzyme-free glucose sensors.

Keywords: surface modification; laser-driven surface alteration; nickel surface; glucose detection; electrocatalytic oxidation

Acknowledgements. *The research is partially funded by the Ministry of Science and Higher Education of the Russian Federation as part of World-class Research Center program: Advanced Digital Technologies (contract No. 075-15-2020-934 dated 17.11.2020).*

Citation: Kondrateva AS, Strekalovskaya DA, Babuyk BV, Kuznetsov A, Filatov LA, Gabdullin PG. Laser induced modification of nickel surface for non-enzymatic glucose detection. *Materials Physics and Mechanics*. 2023;51(4): 107-117. DOI: 10.18149/MPM.5142023_10.

Introduction

Quantitative glucose monitoring is of great world-wide interest because it might significantly diminish the risk of such adverse health effects as various heart trouble, renal failure, or cecity and thus considerably improve the life quality of people with diabetes [1]. Which is one in the SARS-CoV-2 post-pandemic situation, with a large number of diabetic patients infected with COVID-19, has enlarged the interest in real-time glucometer devices [2]. In retrospect, elevated levels of glucose in the blood and urine is one of the key occasions of disability or even death. This metabolic malady occurs when blood insulin concentrations fall below 3.9-6.2 μM (fasting glucose level) or 3.9-7.8 μM (2 hours after food ingestion). In the case of using other biological fluids (sweat, tear, or saliva [3–9]) as analytes, it is necessary to determine significantly lower glucose concentrations: 0.02-0.6, 0.1-0.6, and 0.05-1 μM , respectively. It takes 15-30 minutes to establish a steady-state concentration when analyzing sweat or tear liquid. In the case of

saliva investigation, the measured glucose level can be immediately correlated with that in blood. Generally, methods such as mid-infrared spectroscopy, liquid spectrophotometry, and voltamperometry are applied for glucose levels monitoring, and the choice is made taking into account the specifics of each of the approaches. Among the mentioned methods, electrochemical approach offers the advantages of high accuracy, facile scalability, and ease of analysis of the received measurement signal.

The conventional model of glucose oxidation can be described as follows: at low potentials, the process begins with the anomeric carbon's hydrogen removing. A gluconate ion is formed on the surface at low potentials, while the formation of δ -gluconolactone corresponds to high potentials. As a result of particle desorption and subsequent hydrolysis, only the gluconate remains in the solution [10]. The electrocatalysis process starts with the analyte's adsorption on the electrode surface [11–13]. The superficies of the sensing area play a crucial role [14]. Pletcher suggested that the catalytic process of hydrogenation occurs contemporaneously with the organic substances adsorption. Indeed, the elimination of the hemiacetal hydrogen is presumed to be the limiting step in glucose electrooxidation [15]. In addition, chemisorbed hydroxyl radicals are supposed to participate in the slow stage of the process [16]. Thus, non-enzymatic glucose determination is a pH-controlled process, and OH-containing fluids are suitable for it. This is the reason for the higher sensitivity of non-enzymatic glucose sensors in higher pH environments. Consequently, both electronic and geometric factors must be considered in the manufacture and study of electrocatalysts to take full advantage of the possible improvements of the sensor from the kinetics point of view.

Among various materials [17–18], nickel-oxide-based structures with a developed surface have attracted considerable interest due to their sufficient susceptibility and selectivity to D-(+)-glucose detection. The oxidative activity of nickel-based materials in the glucose determination arises as a result of the rapid transformation of NiO / NiOOH redox pairs formed on the top of electrode surfaces in fluids. Nickel trivalent particles act as the catalyst in the oxidation reaction, which produces a flux of electrons into the surface. However, since nickel oxides and oxyhydroxides have high electrical resistivity, it is often precipitated on the electrode surface. Nevertheless, this additional layer has ensured more efficient electron transfer [19]. Despite the high sensitivity of nickel oxide and advanced state of knowledge regarding the catalytic reactions on its surface, fabrication of sensing metal-based nanostructures mostly requires aggregate chemical synthesis and time-consuming and expensive production techniques.

A wide spectrum of NiO layer formation techniques has been investigated including physical (magnetron sputtering, pulsed laser deposition, thermal deposition), and chemical (reactive evaporation, spray pyrolysis, and chemical vapor deposition) approaches [20]. All proposed methods require a large amount of time: from several hours to days (if additional post-processing is required). Among the various techniques of laser-driven local alteration of metal, foils make it possible to overcome aforementioned disadvantage, providing the possibility of direct formation of functional coatings on Ni electrode surface. According to Wagner's model, as a result of laser radiation and thick metal layer interaction, a parabolic profile of oxygen penetration into the layer is formed [21]. Laser-driven oxidation methods make it possible to obtain almost any thermodynamic stable metal oxides and gradient layers with thicknesses up to 200 μm [22].

The paper analysis indicates that publications on electrocatalysts for amperometric glucose detection in the overwhelming majority of cases do not resemble scientific research in the field of synthesis of new substances. There are no usual attributes, such as patterns of morphology and phase characteristics from the synthesis conditions, kinetic patterns, chemical and phase analysis, the relationship of the surface structure with the material's analyte sensitivity, the proposal of synthesis models, or the response to the disturbance (here

electrocatalytic properties) of the material and their verification, etc. A feature of this work is the choice of the laser-driven surface alteration as a technology that makes it possible to vary the synthesis conditions over a wide range. The main goal of this paper is to estimate how the structure and composition effects on the catalytic properties of the nickel-based materials for potential use in enzymeless measurements of glucose by the electrochemical method.

Methods

Sodium hydroxide (NaOH) pellets (99.5 %), D-(+)-glucose (99.5 %) were purchased from Vecton LLC. Both background and stock solutions of glucose were prepared by dissolving the reagents in deionized water. Nickel foil (99.6 %) sample with a working size of 10 mm. sq. was supplied by Contact LLC.

A novel laser-driven surface alteration technique for non-enzymatic glucose sensor's working electrode preparation was used. Laser processing of the Ni foil was carried out using a pulsed laser (Minimarker-2, CNI LOT) generating 1064 nm wavelength with a pulse duration of $4 \div 200$ ns. The beam profile followed a Gaussian distribution with a spot of 1 mm and a repetition frequency of 30 kHz, resulting in 50 % overlap. Laser energy fluence was from 30 to $240 \text{ mJ}\cdot\text{cm}^{-2}$. The experiments were made in the atmospheric air at ambient temperature. For cyclic voltammetry (CV) experiments, the backsides of samples were passivated by rosin, with a $10 \times 10 \text{ mm}^2$ window.

All electrochemical measurements were performed using electrochemical potentiostat VersaStat 4 Princeton Applied Research. For CV measurements, a three-electrode system has been employed. NiO-Ni sample was used as a working electrode, Pt wire was used as a counter electrode, a silver-chloride electrode (Ag/AgCl) with a KCl solution was used as a reference electrode. The Ag/AgCl reference electrode was separated from the electrochemical cell with 0.1 M NaOH electrolyte using a salt bridge. CV curves were scanned with different voltage scan rates varying between 3 and $80 \text{ mV}\cdot\text{s}^{-1}$ under magnetically stirred conditions. Recording the CV scans repeatedly up to 3000 cycles showed high stability of the studied electrode.

A detailed description of the methodology, choice of modes and materials is presented in more detail in a previously published work [26].

Results and Discussion

SEM images of the boundary between the processed and unprocessed (pristine) regions of a nickel electrode are given in Fig. 1. The pristine region is essentially a smooth Ni surface. It can be seen that the treatment by laser irradiation results in alteration of the surface. EDX analysis indicates that the laser-induced modification added to a change of Ni/O ratio on the surface from $95.96 \pm 0.04/4.04$ to $92.02 \pm 0.06/7.98$, which is evidence of surface oxidation induced by laser irradiation in an oxygen-containing medium. This evidence is also supported by the results of Raman spectroscopy.

The Raman spectra are shown in Fig. 2. For the processed metal, characteristic NiO peaks are observed with maxima at 512 cm^{-1} (longitudinal optical vibrations, LO, which is due to the presence of defects and is absent in the spectrum of crystalline NiO according to [23] and 960 cm^{-1} (2LO) [24] alongside peaks related to carbon inclusions ($1332, 1601, 2920 \text{ cm}^{-1}$), the latter probably due to surface contamination of the sample with carbon [25]. Thus, the described laser modification of the nickel surface leads to the formation of an oxide layer.

Although the nickel foil treatment was carried out in an atmosphere containing about 20 % oxygen, the amount of oxygen in the altered layer remains rather low. This may be due to the peculiarities of the selected mode of surface alteration when a protective atmosphere of evaporated nickel was formed during laser treatment, which prevented the penetration of oxygen to the surface. In this case, evaporation and condensation of the material occurred,

which did not lead to its significant loss. This is confirmed by the SEM results, which show the absence of porous structures.

The SEM and Raman spectroscopy results indicate the fundamental possibility of producing oxide layers in solution through the described laser-driven surface alteration. The considered fabrication method makes it possible to obtain a developed oxidized metal surface quickly and reproducibly.

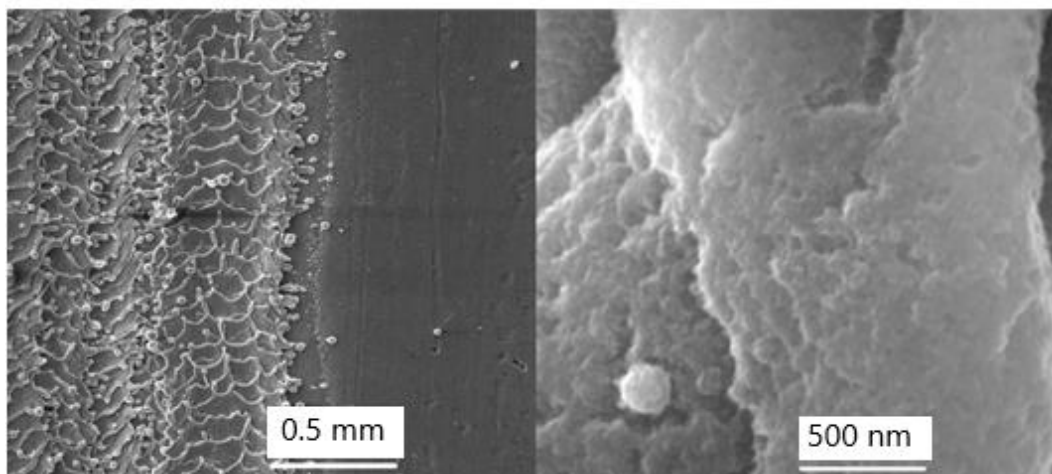


Fig. 1. SEM images of vicinities of the boundary between the processed and unprocessed regions of a nickel electrode surface at different magnifications

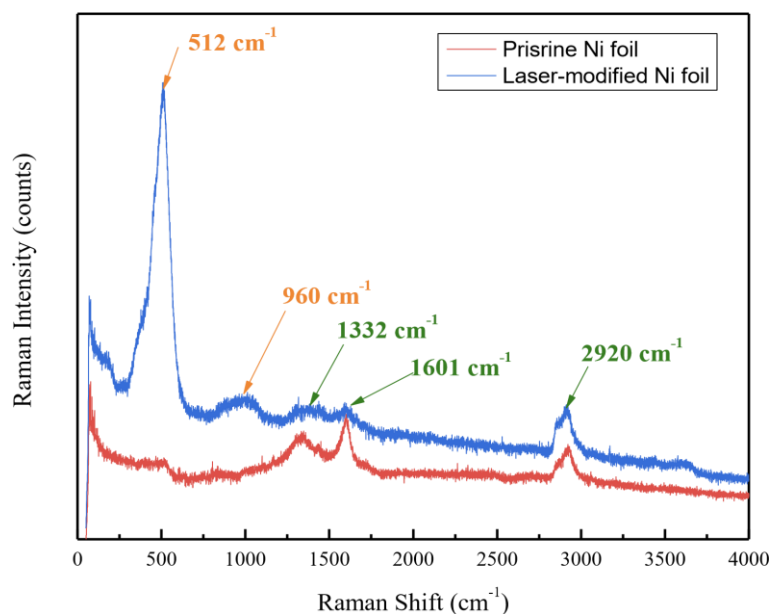


Fig. 2. Raman spectra obtained from the boundary region between the processed and unprocessed areas of a nickel electrode

Study of the electrooxidative activity of pristine Ni foil. At the first stage, the behavior of pristine Ni foil in 0.1M NaOH was studied. The characteristic peaks of the transition Ni (III) / Ni (II) [26] were not observed (Fig. 3). Additional electrochemical treatment (anodic, 1.5 V, 60 s), etching, and mechanical activation of the surface of the initial foil lead to the appearance of transition corresponding peaks on the CV. Upon increasing the analyte concentration from 0.1 to 1.5 μ M, both anodic and cathodic peaks current (Fig. 3, inset) was increased, which can indicate the surface oxidation of glucose molecules. The slight variation

of the anodic and cathodic peak positions is likely due to the crystal structures of the electrochemical formed surface layers change [27,28].

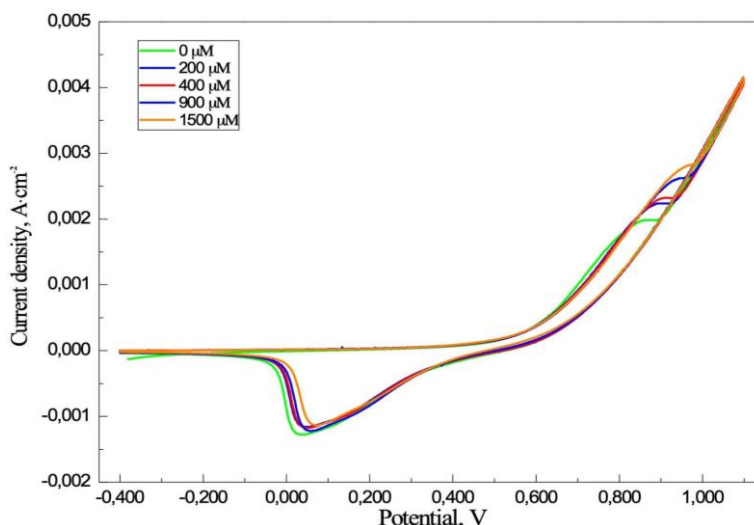


Fig. 3. Cyclic voltammograms of pristine Ni and NiO in 0.1 M NaOH solutions at scan rate of $20 \text{ mV}\cdot\text{s}^{-1}$

The most likely reaction scheme can be supported by electrochemical activation of NiO followed by the redox reactions on the NiOOH surface, which were discussed elsewhere [29,30]. On the NiOOH surface, glucose oxidizes to gluconolactone which reacts with a water molecule to form gluconate and hydronium ions.

Study of the electrooxidative activity of modified NiO–Ni layer toward glucose. For non-enzymatic sensing study, CV measurements have been carried out with NiO–Ni sample as the working electrode at a scan rate of $20 \text{ mV}\cdot\text{s}^{-1}$ in the presence and absence of glucose, in the 0.1 M NaOH electrolyte as demonstrated in Fig. 4. When a preliminary laser-activated nickel foil is used as a working electrode in 0.1 M NaOH media, characteristic peaks of the Ni (III) / Ni (II) transition are observed on CV at potentials of about 0.4 V. In the region of high glucose level, an anodic peak intensity decrease is also observed. It is likely due to the poisoning of the work surface. In this case, the intensity observed for laser-modified nickel is higher than for the oxide formed by anodic treatment.

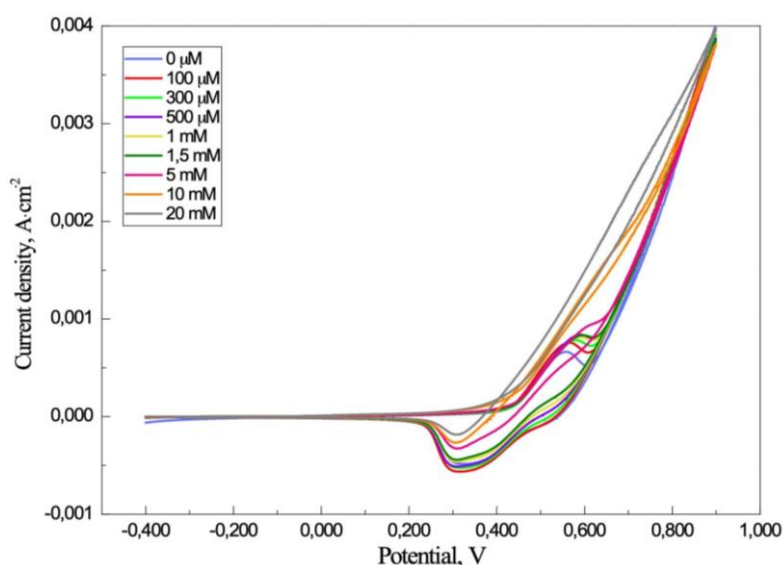


Fig. 4. Cyclic voltammograms of NiO–Ni sensitive layer in 0.1 M NaOH solutions in the presence of D-(+)-glucose concentrations up to 20 mM

The effect of scan rate on the anodic and cathodic peaks current (I_a and I_c) of 1 μM D-(+)-glucose was measured in the range of 3 to 80 $\text{mV}\cdot\text{s}^{-1}$ (Fig. 5). It was detected that both the anodic and cathodic peaks current (I_a and I_c) gains linearly with the scan rate's square root ($(\text{mV}\cdot\text{s}^{-1})^{1/2}$). The glucose oxidation in those conditions is limited by diffusion. The diffusion coefficient was counted for the pseudo plane electrode in reversible charge transfer mode and was $1.8 \times 10^{-2} \text{ cm}^2\cdot\text{s}^{-1}$. This value is higher than the previously described quantity [31].

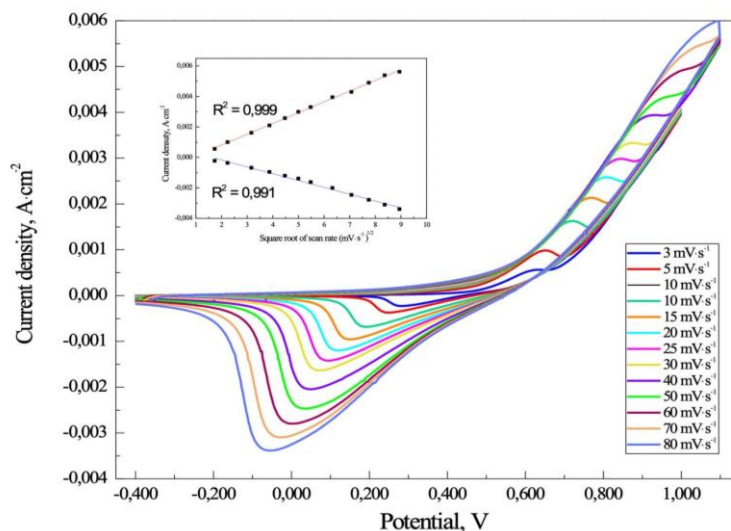


Fig. 5. Cyclic voltammograms of NiO-Ni sensitive layer in 0.1 M NaOH solutions in the presence of 1 μM of D-(+)-glucose at different scan rates. Inset: anodic and cathodic current versus the square root scan rate

Amperometric study for NiO-Ni sensitive layer. The electrocatalytic behavior of the NiO-Ni sensitive layer on glucose oxidation was examined by monitoring a current replication on glucose adjunction at a fixed potential (Fig. 6). Firstly, the working potential was determined by the dropwise adjunction of 0.1 μM glucose in 0.1 M NaOH. At a potential of 0.4 V, a sufficient signal-to-noise ratio, adequate correlation coefficient value, and current response were measured. All results are in an agreement with the corresponding value obtained in [32]. At a potential of 0.4 V, the current response increases linearly with analyte quantity in the range of 0.1 – 1.5 μM . A correlation coefficient is counted to be of 0.996. Taking into account the slope ($0.005 \text{ mA}\cdot\text{mM}^{-1}$) and electrochemical area (1.2 cm^2) of the formed sensitive layer, the susceptibility of the structure was calculated as $0.4 \text{ mA}\cdot\mu\text{M}^{-1}\cdot\text{cm}^{-2}$. The limit of detection (LOD) (0.4 μM) and the limit of quantification (LOQ) (1 mM) also were calculated.

The current value does not diverge from linearity at higher analyte quantity. This fact indicates that neither poisoning of the electrode nor glucose isomers formation is affected, which is an opposite situation compared to that known to occur in high-pH solutions [33], which could be attributed to low D-glucose concentrations. The performance of the reported NiO-Ni structures in the range of 0.6 – 2 μM D-glucose concentration allows us to suggest their use as sensitive elements for determining the glucose level in blood. Usage of the formed structures for the analysis of saliva, tears, or sweat requires improvement of the detection limit and the limit of quantification, for example, by increasing the electrochemical area.

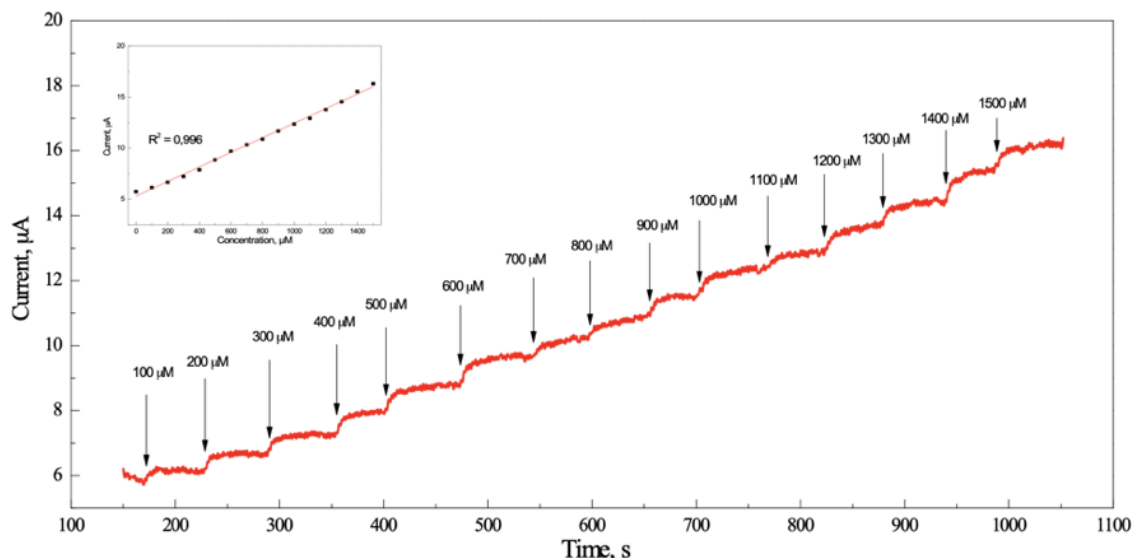


Fig. 6. Amperometry of D-(+)-glucose on NiO-Ni sensitive layer in 0.1 M NaOH solutions with $E_{st} = 0.4$ V under continuous agitation. Inset: the anodic and cathodic peaks current versus the D-(+)-glucose concentration

Table 1 shows the comparison of working detection potentials, sensitivity, LOD, preparation time of the currently prepared NiO-Ni sensitive layer with previously cited nickel-based structures in terms of working potential range, sensitivity, limits of detection, and fabrication complexity. The proposed method of laser modification is a much simpler and faster technique compared to standard methods of sol-gel synthesis, sintering, and pressing. In spite of the simplicity of the proposed NiO-Ni sensitive layer fabrication methodology, it shows comparable D-glucose detection performance. At the same time, the samples obtained using this technology showed comparable sensitivity and detection limits. It is planned to further increase the detection limit and sensitivity of the element by introducing additives of other materials (copper, iron, carbon in various forms), which is planned as a continuation of work on this topic.

Table 1. Comparison of working detection potentials, sensitivity, LOD, preparation time of this work with previously reported studies for glucose detection.

Sensing layer	Working potential, V	Sensitivity, $\text{mA} \cdot \mu\text{M}^{-1} \cdot \text{cm}^{-2}$	LOD, mM	Preparation time, h	Reference
Ni-Cu-Vulcan carbon	0.5	1.5	0.02	10-12	[30]
Ni/Au nanowires	0.6	1.9	0.1	10-12	[34]
$\text{NiCo}_2\text{S}_4/\text{Ni}$	0.45	0.2	6	0.5	[35]
NiO/MWCNT composite	0.5	0.1	0.01	5	[36]
$\text{Ni}(\text{OH})_2$ and NiO	0.58	0.1	0.7	30	[37]
NiO-Ni	0.4	0.6	0.6	1/3	This work

Repeatability and stability of NiO-Ni sensitive layer. Reproducibility and consistency of results are the main parameters for the performance of the device. Cyclic voltammetry is known as a precision and accurate method [38]. Repeatability is an important goal for sensor performance. The reproducibility of the readings of the system under study was studied by

analyzing the CV of three groups of layers, sensitive to NiO-Ni, prepared in different experiments. All samples were investigated under cyclic conditions in a 0.1 M NaOH solution to 0.1 μM D-glucose response with continuous stirring. The Figure 7 shows the averaged data for 6 samples: 3000 cyclic voltammograms, which were obtained on NiO-Ni sensitive layers. Repeatability of standard derivation was measured to be 4 %. It shows that the formed structure is not poisoned by the reaction products formed during the whole course of the process.

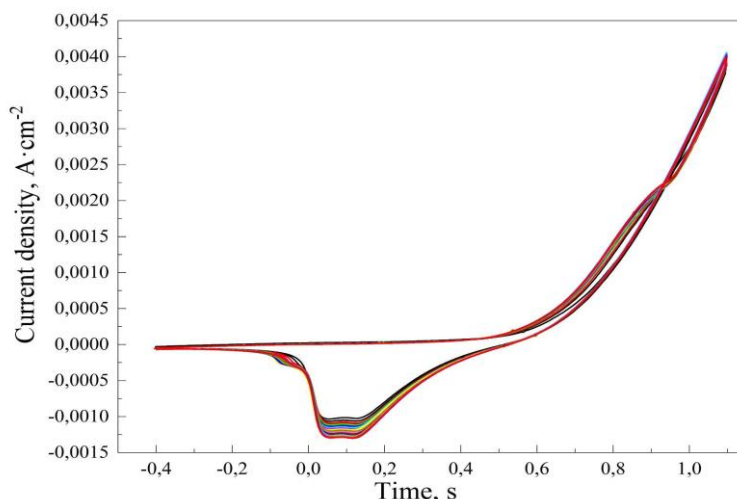


Fig. 7. 3000 cyclic voltammograms of NiO-Ni sensitive layer in 0.1 M NaOH solutions in the presence of 0.1 μM of D-(+)-glucose at scan rate of $50 \text{ mV}\cdot\text{s}^{-1}$

The stability of the prepared oxide layer was also evaluated by keeping a NiO-Ni sensitive layer for 100 days at ambient conditions. The measured current remains 85 % of the initial value after 100 days. This demonstrates that the prepared non-enzymatic glucose sensor has a high shelf-life stability. A decrease in the anodic and cathodic currents during long-term cyclic measurements can be related to the formation of $\gamma\text{-NiOOH}$, in which the volume of the working surface of the electrode increases up to the formation of microcracks. Physical destruction of the working surface is known to occur [39]. The results convincingly indicate the high reproducibility and high stability of the preliminarily prepared sensitive layer of NiO-Ni for the enzyme-free determination of D-(+)-glucose.

Conclusions

Nickel-based oxide nanostructure was formed on a metallic nickel surface by laser-driven modification approach. Formed structures were examined to be sensing electrodes for non-enzymatic glucose detection. The formed NiO-Ni structure morphology and chemical composition were investigated. Electrochemical analysis of NiO-Ni electrode behavior in alkaline solution confirmed the glucose-sensitive oxide layer to be presented on the top of the electrode. The electrochemical glucose detection results indicate enhancement of the electrode performance after laser modification as compared to Nickel foil.

A linear sensitivity of $0.4 \text{ mA}\cdot\mu\text{M}^{-1}\cdot\text{cm}^{-2}$ with a correlation coefficient of 0.996 was obtained. Reproducibility and stability of the proposed non-enzymatic D-(+)-glucose sensor were established by long-term measurements. These results reveal the potentiality of producing advanced functional materials (in the present case, NiO-Ni structures with a modified surface) for competitive glucose sensors by implementing low-cost lasers to perform the metal oxidation and surface activation processes.

References

1. Kang S, Zhao K, Yu DG, Zheng X, Huang C. Advances in biosensing and environmental monitoring based on electrospun nanofibers. *Advanced Fiber Materials*. 2022;4(3): 404–435.
2. Levshakova AS, Khairullina EM, Panov MS, Ninayan R, Mereshchenko AS, Shishov A, Tumkin II. Modification of nickel micropatterns for sensor-active applications from deep eutectic solvents. *Optical and Quantum Electronics*. 2023;55(3): 267.
3. Bariya M, Nyein HY, Javey A. Wearable sweat sensors. *Nat. Electron*. 2018;1: 160–171.
4. Kim J, Campbell AS, de Ávila BE, Wang J. Wearable biosensors for healthcare monitoring. *Nat. Biotechnol*. 2019;37(4): 389–406.
5. Mannoor MS, Tao H, Clayton JD, Sengupta A, Kaplan DL, Naik RR, Verma N, Omenetto FG, McAlpine MC. Graphene-based wireless bacteria detection on tooth enamel. *Nat. Commun*. 2012;3(1): 763.
6. Wei M, Qiao Y, Zhao H, Liang J, Li T, Luo Y, Lu S, Shi X, Lu W, Sun X. Electrochemical non-enzymatic glucose sensors: Recent progress and perspectives. *Chem. Commun*. 2020;56(93): 14553–14569.
7. Qiao Y, Liu Q, Lu S, Chen G, Gao S, Lu W, Sun X. High-performance non-enzymatic glucose detection: using a conductive Ni-MOF as an electrocatalyst. *Journal of Materials Chemistry B*. 2020;8(25): 5411–5415.
8. Wang Z, Cao X, Liu D, Hao S, Kong R, Du G, Asiri AM, Sun X. Copper-nitride nanowires array: an efficient dual-functional catalyst electrode for sensitive and selective non-enzymatic glucose and hydrogen peroxide sensing. *Chemistry—A European Journal*. 2017;23(21): 4986–4989.
9. Liu Y, Cao X, Kong R, Du G, Asiri AM, Lu Q, Sun X. Cobalt phosphide nanowire array as an effective electrocatalyst for non-enzymatic glucose sensing. *Journal of Materials Chemistry B*. 2017;5(10): 1901–1904.
10. Hwang DW, Lee S, Seo M, Chung TD. Recent advances in electrochemical non-enzymatic glucose sensors—a review. *Analytica Chimica Acta*. 2018;1033: 1–34.
11. Heller A, Feldman B. Electrochemical glucose sensors and their applications in diabetes management. *Chemical Reviews*. 2008;108(7): 2482–2505.
12. Pletcher D. Electrocatalysis: present and future. *J. Appl. Electrochem*. 1984;14(4): 403–415.
13. Tian K, Prestgard M, Tiwari A. A review of recent advances in nonenzymatic glucose sensors. *Materials Science and Engineering: C*. 2014;41: 100–118.
14. Kokkindis G, Leger JM, Lamy C. Structural effects in electrocatalysis: oxidation of D-glucose on pt (100),(110) and (111) single crystal electrodes and the effect of upd adlayers of Pb, Tl and Bi. *Journal of Electroanalytical Chemistry and Interfacial Electrochemistry*. 1988;242(1-2): 221–242.
15. Hsiao MW, Adžić RR, Yeager EB. Electrochemical oxidation of glucose on single crystal and polycrystalline gold surfaces in phosphate buffer. *Journal of the Electrochemical Society*. 1996;143(3): 759.
16. Pessoa AM, Fajín JL, Gomes JR, Cordeiro MN. Ionic and radical adsorption on the Au (hkl) surfaces: A DFT study. *Surface Science*. 2012;606(1-2): 69–77.
17. Niu Q, Lu W, Bao C, Wei M, Chen ZA, Jia J. Glucose-sensing abilities of mixed-metal (NiCo) Prussian blue analogs hollow nanocubes. *Journal of Electroanalytical Chemistry*. 2020;874: 114507.
18. Bariya M, Shahpar Z, Park H, Sun J, Jung Y, Gao W, Nyein HY, Liaw TS, Tai LC, Ngo QP, Chao M. Roll-to-roll gravure printed electrochemical sensors for wearable and medical devices. *ACS Nano*. 2018;12(7): 6978–6987.

19. Mahadevan A, Fernando S. Inorganic iron-sulfur clusters enhance electron transport when used for wiring the NAD-glucose dehydrogenase based redox system. *Microchimica Acta*. 2018;185: 1–8.
20. Kondrateva AS, Mishin M, Shakhmin A, Baryshnikova M, Alexandrov SE. Kinetic study of MOCVD of NiO films from bis-(ethylcyclopentadienyl) nickel. *Physica Status Solidi (C)*. 2015;12(7): 912–917.
21. Atkinson A. Transport processes during the growth of oxide films at elevated temperature. *Reviews of Modern Physics*. 1985;57(2): 437.
22. Nánai L, Vajtai R, George TF. Laser-induced oxidation of metals: state of the art. *Thin Solid Films*. 1997;298(1-2): 160–164.
23. George G, Anandhan S. Synthesis and characterisation of nickel oxide nanofibre webs with alcohol sensing characteristics. *Rsc Advances*. 2014;4(107): 62009–62020.
24. Bose P, Ghosh S, Basak S, Naskar MK. A facile synthesis of mesoporous NiO nanosheets and their application in CO oxidation. *Journal of Asian Ceramic Societies*. 2016;4(1): 1–5.
25. Guedes-Silva CC, Rodas AC, Silva AC, Ribeiro C, Carvalho FM, Higa OZ, Ferreira TD. Microstructure, mechanical properties and in vitro biological behavior of silicon nitride ceramics. *Materials Research*. 2018;21(6): e20180266.
26. Kondrateva A, Babuyk V, Strekalovskaya D, Filatov L, Gabdullin P, Kvashenkina O, Prokopenko Y, Gruzdev A, Petruhno K, Kuznetsov A. Laser-driven metal alteration for glucose detection sensor. *Materials Physics and Mechanics*. 2021;47(5): 767–779.
27. Zhao C, Shao C, Li M, Jiao K. Flow-injection analysis of glucose without enzyme based on electrocatalytic oxidation of glucose at a nickel electrode. *Talanta*. 2007;71(4): 1769–1773.
28. Kwan KW, Hau NY, Feng SP, Ngan AH. Electrochemical actuation of nickel hydroxide/oxyhydroxide at sub-volt voltages. *Sensors and Actuators B: Chemical*. 2017;248: 657–664.
29. Fleischmann M, Korinek K, Pletcher D. The oxidation of organic compounds at a nickel anode in alkaline solution. *Journal of Electroanalytical Chemistry and Interfacial Electrochemistry*. 1971;31(1): 39–49.
30. Nisar S, Tariq M, Muhammad S, Saqib M, Akbar F. Electrocatalytic efficacy of Ni-Cu@VC-72: Non-enzymatic electrochemical detection of glucose using Ni-Cu nanoparticles loaded on carbon black. *Synthetic Metals*. 2020;269: 116578.
31. Kim S, Muthurasu A. Metal-organic framework–assisted bimetallic Ni@Cu microsphere for enzyme-free electrochemical sensing of glucose. *Journal of Electroanalytical Chemistry*. 2020;873: 114356.
32. Zhang X, Wang Y, Ning X, Chen J, Shan D, Gao R, Lu X. Three-dimensional porous self-assembled chestnut-like nickel-cobalt oxide structure as an electrochemical sensor for sensitive detection of hydrazine in water samples. *Analytica Chimica Acta*. 2018;1022: 28–36.
33. Shamsipur M, Najafi M, Hosseini MR. Highly improved electrooxidation of glucose at a nickel (II) oxide/multi-walled carbon nanotube modified glassy carbon electrode. *Bioelectrochemistry*. 2010;77(2): 120–124.
34. Qin L, He L, Zhao J, Zhao B, Yin Y, Yang Y. Synthesis of Ni/Au multilayer nanowire arrays for ultrasensitive non-enzymatic sensing of glucose. *Sensors and Actuators B: Chemical*. 2017;240: 779–784.
35. Babu KJ, Raj Kumar T, Yoo DJ, Phang SM, Gnana Kumar G. Electrodeposited nickel cobalt sulfide flowerlike architectures on disposable cellulose filter paper for enzyme-free glucose sensor applications. *ACS Sustainable Chemistry & Engineering*. 2018;6(12): 16982–16989.
36. Prasad R, Bhat BR. Multi-wall carbon nanotube–NiO nanoparticle composite as enzyme-free electrochemical glucose sensor. *Sensors and Actuators B: Chemical*. 2015;220: 81–90.

37. Pal N, Banerjee S, Bhaumik A. A facile route for the syntheses of Ni (OH) 2 and NiO nanostructures as potential candidates for non-enzymatic glucose sensor. *Journal of Colloid and Interface Science*. 2018;516: 121–127.
38. Lerke SA, Evans DH, Feldberg SW. Digital simulation of the square scheme in cyclic voltammetry: A comparison of methods. *Journal of Electroanalytical Chemistry and Interfacial Electrochemistry*. 1990;296(2): 299–315.
39. Singh D. Characteristics and effects of γ -NiOOH on cell performance and a method to quantify it in nickel electrodes. *Journal of the Electrochemical Society*. 1998;145(1): 116.

THE AUTHORS

Kondrateva A.S. 

e-mail: freyanasty@ya.ru

Babuyk B.V.

e-mail: vladislavbabyuk@gmail.com

Filatov L.A.

e-mail: balldr@mail.ru

Strekalovskaya D.A. 

e-mail: darya.strek@gmail.com

Kuznetsov A.

e-mail: leshiy2698@mail.ru

Gabdullin P.G. 

e-mail: pavel-gabdullin@yandex.ru